

Applications of uncertainty quantification in energy

Jeroen A.S. Witteveen

Center for Mathematics and Computer Science (CWI)

Science Park 123

1098XG Amsterdam

The Netherlands

jeroen.witteveen@cw.nl

ABSTRACT

Non-intrusive Uncertainty Quantification (UQ) has the advantage that it can readily be applied to many different problems. Here the focus is mainly on the results of successful applications of uncertainty quantification in energy. Renewable electrical energy sources are necessary to reduce our current dependence on fossil fuels. However, the output of sustainable energy technologies such as wind turbines and Photo-Voltaic (PV) systems are uncertain due to their dependence on the weather conditions. This and their typically distributed generation increases the uncertainty also for electrical grid operators. In addition, the safety of generating electricity in nuclear reactors is vital in the presence of uncertainties. The uncertainty quantification and robust optimization of a wind turbine, a stochastic power flow, a nuclear reactor safety flow, and a wind engineering example are discussed.

Contents

1.0 Introduction	1
2.0 Wind turbine flow	2
3.0 Stochastic power flow	3
4.0 Nuclear reactor safety flow	7
5.0 Wind engineering	8
6.0 Conclusions	10

1.0 INTRODUCTION

Uncertainties play an important role in many branches of computational science. Non-intrusive Uncertainty Quantification (UQ) has the advantage that it can readily be applied to many different problems. Non-intrusive UQ methods are based on performing multiple deterministic simulations for different values of the uncertain

parameters inside their range. They therefore re-use the deterministic equations and they can be coupled to existing computer codes. This approach does in principle not fundamentally depend on the specific physics that is modeled. Next to Computational Fluid Dynamics (CFD), UQ has for example recently been applied to neuro-dynamics and enzymatic reaction equations from the life sciences and the Heston model for pricing stocks and options under risk-neutral measure in computational finance [9]. Here we focus mainly on the results of successful applications of uncertainty quantification in energy.

Most of our electrical energy is still being generated today by burning fossil fuels. This is clearly an exhaustible and finite resource of energy, of which the cost price will continue to rise into the long-term future. It will therefore negatively impact the economic growth and, as a consequence, the prosperity and the standard of living of the next generations. These conventional energy sources can also affect the global climate and the local environment. Our current dependence on oil products in particular makes us vulnerable for the influence of a small number of foreign country suppliers as well.

Therefore, governments world wide are actively stimulating the research and development of sustainable energy alternatives. Wind power are the fastest growing form of renewable energy owing to the increasing turbine sizes and the construction of extensive new wind farms. The related scientific attention focuses especially on innovations in wind power technology at sea. The additional technological challenges in the maritime environment and the reduction of the relatively higher costs need original solutions. An impressive number of large-scale offshore wind farms and experimental test sites are currently already being installed.

Offshore wind turbines have the advantage that there are higher wind speeds at sea and that they do not cause inconveniences to residents. On the other hand, the cost of offshore wind energy is three times as high as the current electricity market price. Offshore wind turbines are, for instance, built in large offshore wind farms to decrease installation and maintenance costs. However, the presence of the other wind turbines can reduce the total power production of a wind farm up to 40%, if the turbines are in each other's wake.

However, a major problem of wind power is the variability in the electricity production of wind turbines. These fluctuations are caused, for instance, by the atmospheric wind conditions as well as other uncertainties that can more easily be controlled. Examples of this second type of uncertainties are the effect of production tolerances on the blade geometry and the decreasing efficiency of wind turbines due to wear and tear over their lifetime. As a consequence, the availability of wind power is much less predictable than that of traditional energy sources. The increasing implementation and the distributed generation of wind power, therefore, poses a number of specific new challenges on the management of the electrical grid. The generation and the demand of electricity have to be in balance at all times in order to avoid the destabilization of the frequency and the voltage equilibrium on the grid. A large amount of experience has accumulated over the last decades in the accurate prediction of the daily consumer electricity demand. Conventional power plants can be scheduled to compensate for these anticipated slow changes on the demand side. However, they are not designed to respond to the high-frequency fluctuations in wind power generation.

Below, we will first consider UQ of an individual wind turbine in Section 2.0. The impact of uncertain renewable energy on the electrical grid is studied in Section 3.0. In Section 4.0, Nuclear Reactor Safety (NRS) flows are considered, in which the quantification of uncertainties obviously plays also an important role. Finally, a wind engineering application is considered in Section 5.0 in the form of a 5:1 rectangular cylinder. The main conclusions are summarized in Section 6.0.

2.0 WIND TURBINE FLOW

Quantification of the uncertainties for a wind turbine and its robust design optimization under uncertainties is considered in [6, 7]. The considered baseline case is the 50kW AOC 15/50 wind turbine at the Acqua Spruzza

site in Italy, for which wind data is available. Next to the wind conditions, uncertainty is also considered in the surface roughness due to the accumulation of insect impacts on the blade, and geometrical manufacturing tolerances. The probability densities of the wind conditions are shown in Figure 1 for the wind magnitude, the turbulence intensity, and the wind direction. The effect of insect contamination on the flow transition is modeled by modifying the e^N factor in the transition model, with a uniform distribution for $N \sim U(1, 9)$. Manufacturing tolerances are incorporated in terms of a uniform distribution of the blade twist angle $\theta \sim U(-2, 2)$. Both insect contamination and manufacturing tolerances are modeled by three uncertain parameters at the root, mid-span, and tip region of the blades.

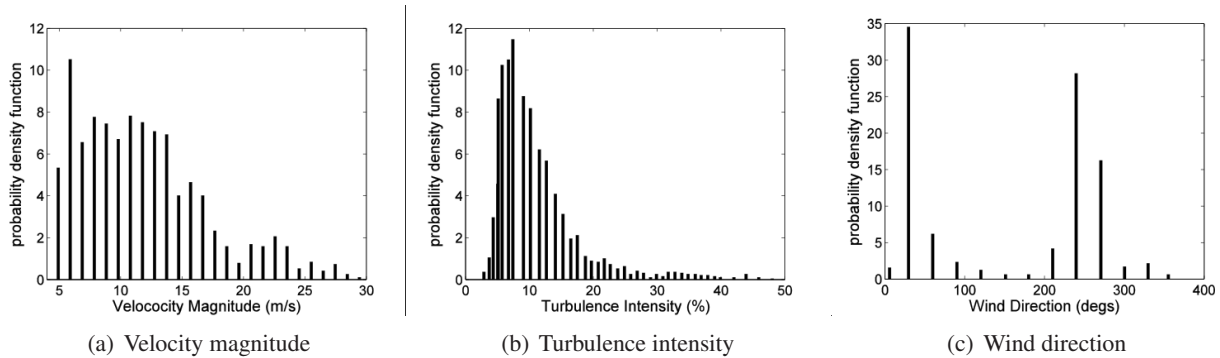


Figure 1: Input probability density functions for the uncertain wind conditions [6].

The uncertainty propagation is performed by coupling the multi-physics code suite EOLO [7] for aero-elastic-acoustic wind turbine modeling with the non-intrusive solution-adaptive Simplex Stochastic Collocation approach [12, 13] in an iterative way. The wind uncertainty has the largest impact on the wind turbine performance in terms of the power output coefficient with a mean and standard deviation of 0.2776 and 0.1189 compared to a deterministic output of 0.4596. Insects and manufacturing have an appreciably smaller impact with a mean and standard deviation of 0.4340 and 0.0162, and 0.4560 and 0.0071, respectively. The wind uncertainty halves the output compared to the deterministic performance.

Therefore, an optimization under uncertainties is performed in [7]. The green and flat Probability Density Function (PDF) in Figure 2 shows the trade-off of the deterministic optimization of the turbine between performance and noise. The orange and peaked distribution is the PDF after robust optimization including the effect of the uncertainties. It shows that the robust optimum has a peak probability at the peak performance in the range of that distribution. The distribution is also significantly narrower than the deterministic optimum. As a consequence the robustly optimized design will show a more stable performance at its maximum despite the presence of uncertainties.

3.0 STOCHASTIC POWER FLOW

Transmission System Operators (TSOs) find they have to deal with increasing uncertainty in their network planning and operation processes. This uncertainty can be seen “over time”, such as the uncertainty of the output of a wind power plant due to the variability of wind as an energy resource. The alternate perspective is uncertainty “in scenario”, for example the choice of connection location or the size and composition of a generation portfolio to be considered in planning studies.

Factors contributing to the increase in uncertainty are market liberalization, the introduction of renewable generation in response to the need for environmental conservation and the decentralization of generation and

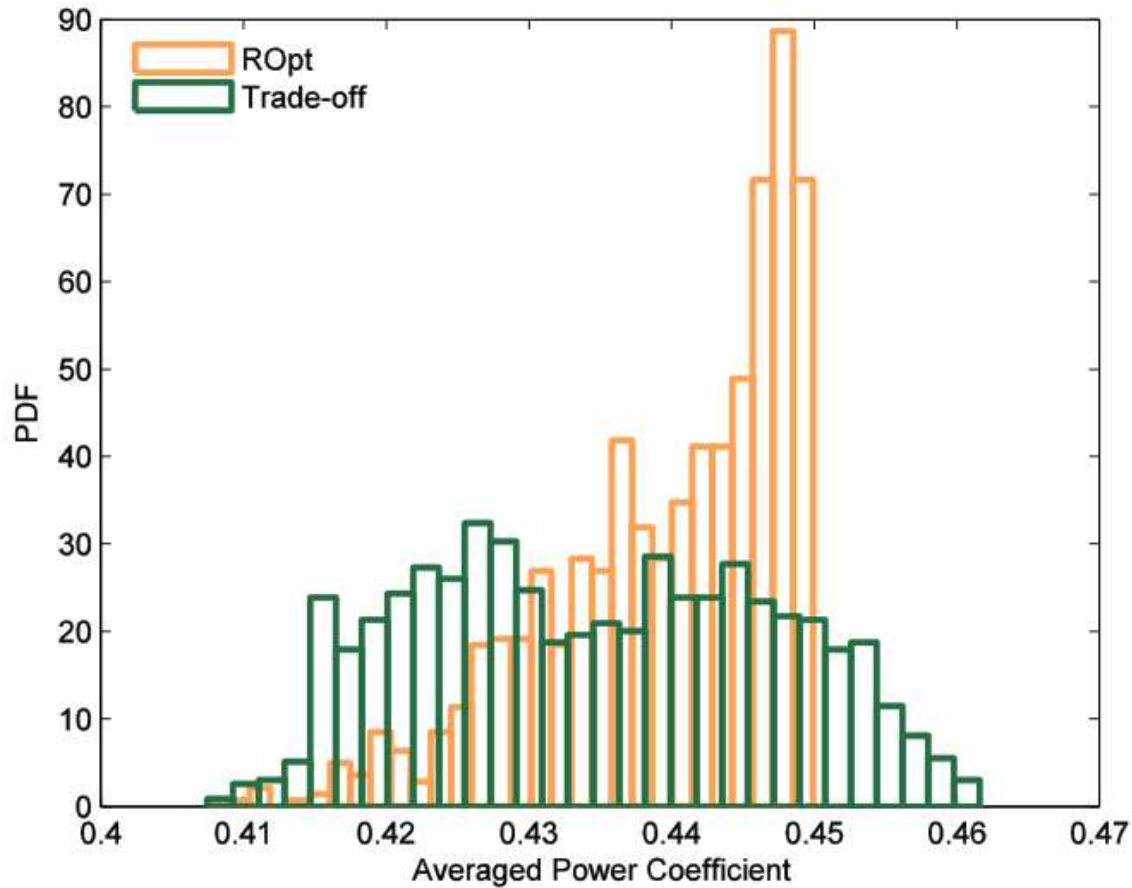


Figure 2: Probability density of power coefficient for optimum and trade-off design [7].

(in future) demand control. Market liberalization has an impact on both network capacity (long-term) and operational (daily) planning. Information about where a power plant will be built is commercially sensitive and therefore less easily available in capacity planning. Also, modern (renewable) power plants can be built in times far shorter than the time needed for developing network assets. In operations, market liberalization causes decisions about committing generation or demand being taken on non-technical grounds and closer to the gate closing time of the network control period. By consequence, there is less time to verify system adequacy. The increased price volatility of the market-based system leads to more variable generation and demand commitment (e.g. of glasshouse-based combined-cycle generation and industrial gas turbines), in turn leading to a more variable power transmission requirement.

The development of wind power and Photo-Voltaic (PV) solar power technology introduced generation to the electricity system that is either non-controllable or reduced-observable, or both. These technologies are mature and have reached a scale where they impact the planning and operation of the system. Wind and PV power plants are however being developed not only as large-scale installations, but also as small house-hold size units. This is leading to the connection of very large numbers of decentralized generators that, besides being poorly or non-controllable, are also less observable for the TSO: their output balances with the local demand

and cannot be easily distinguished thereof.

It is in this environment that the TSO has to perform planning processes. The common method to deal with all the uncertainties is to capture them in a (large but limited) number of scenarios. In this way the traditional network analysis tools can be used and the planning process remains transparent i.e. understandable also for outsiders like the regulator and the general public. The bottlenecks found in the results of the traditional network analyses are weighed in terms of risk. Mitigation measures, often construction projects, are developed for those bottlenecks (or a group of bottlenecks) that are perceived as a relevant risk.

This planning methodology, no matter how sophisticated, has a fundamental short coming: it relies on the engineers subjective perception of risk in both definition of scenarios on the input and the weighing of the threat of a bottleneck on the output. It would help if the traditional power system analysis techniques and tools could cope with the uncertainty by incorporating it in the power system model.

We formulate the stochastic power flow problem in terms of an uncertainty quantification problem with probability distributions for the uncertain inputs. The uncertainty quantification problem is solved using the Stochastic Collocation method [15]. We present the results of a case study combining Stochastic Collocation with conventional power system analysis software.

A power flow model was developed in PSS/E 33 for the 300 bus 411 branch IEEE network [10]. A single line diagram of the power system is shown in Figure 3. We defined all generators in this system as being either conventional, wind power plants or PV power plants for the arbitrarily chosen totals as listed in Table 1. The generation by the conventional power plants was adjusted to balance the demand. The steady-state power flow equations are solved for the bus voltages and the branch currents through the transmission lines.

Table 1: Generation in test case grid

Generation	Installed capacity in MW	%
Conventional	18303	79
Wind	3894	17
PV	1003	4
Total	23200	100

The stochastic properties of the wind and PV power generators, and of the demand in the system, are shown in Figure 4. The Probability Density Function (PDF) of the offshore wind speed in the Netherlands at a height of 90 m can be formulated as a Weibull distribution with scale factor $\lambda = 10$ and shape factor $k = 2.2$ [4]. The distribution function of the active power output of the wind power plants is obtained through combining this wind speed distribution with a standard turbine power curve. The PDF for the scale factor from the PV power plants is obtained using as input the yearly average hourly solar irradiation values in the Netherlands [4]. The output of the PV systems in the grid is assumed to depend linearly on the solar irradiation PDF. The third uncertainty incorporated in the power system model is the variation in demand over the 24 hours of a day and over the days of the week. Realistically one should discriminate load classes (industry, households), but for this proof-of-principal study this was simplified to one distribution function. This distribution function is based on historical data of the 15-minute average active power demand of Dutch households [11].

The resulting Cumulative Distribution Function (CDF) for the current through branch 1 is shown in Figure 5 for tensor and sparse grid Stochastic Collocation on levels 0 to 3. The number of simulations required for the tensor and sparse grids are, respectively, $n_s = \{1, 27, 125, 729\}$ and $n_s = \{1, 7, 25, 69\}$. The predictions are compared to a Monte Carlo simulation of 10,000 power flow computations. The Stochastic Collocation CDFs are generated by evaluating the same points on the polynomial response surface approximation. The figures show that a level 1 tensor grid with 27 points and a level 2 sparse grid with 25 points give accurate results. So,

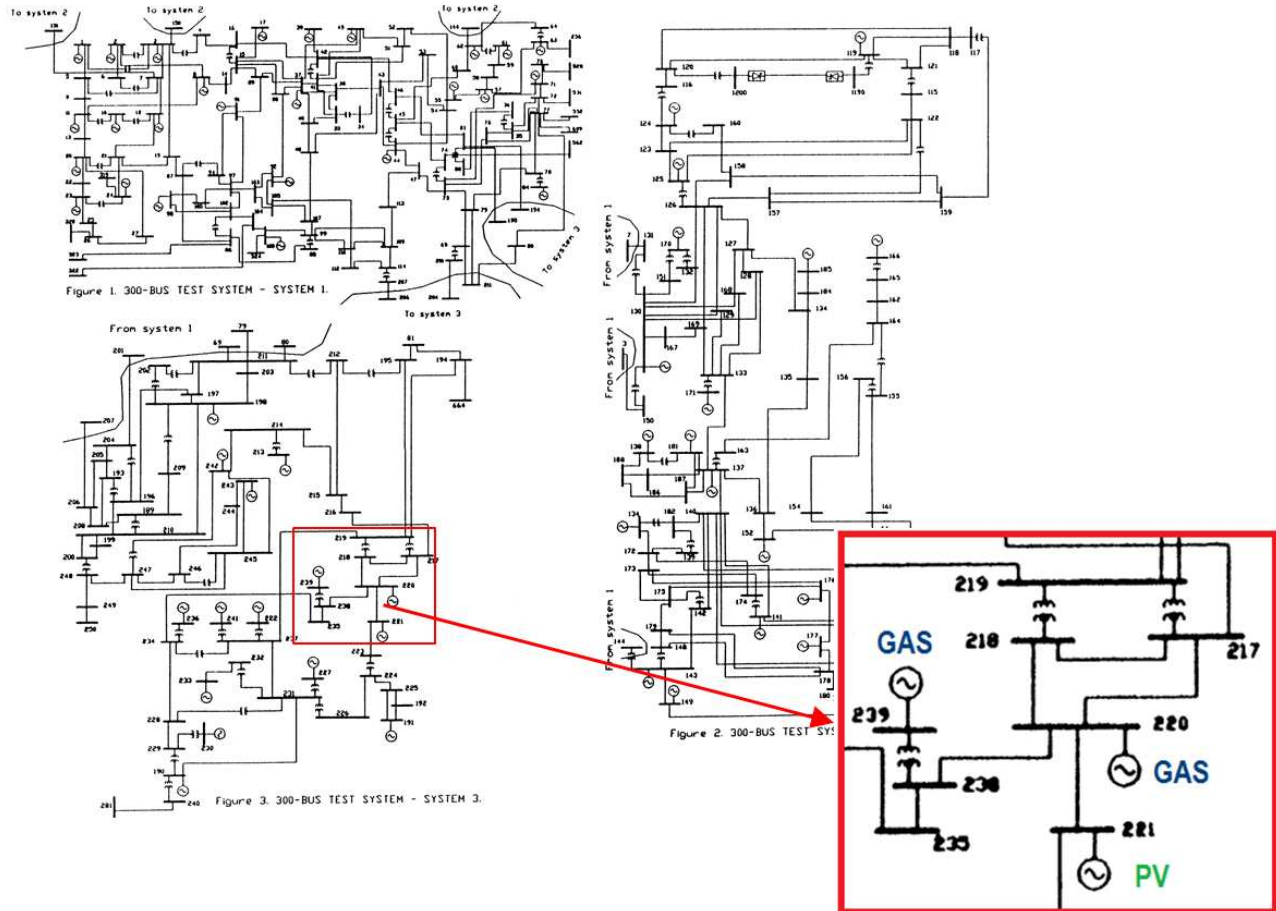


Figure 3: Single line diagram of the IEEE 300 bus test system with example of generator type classification [10].

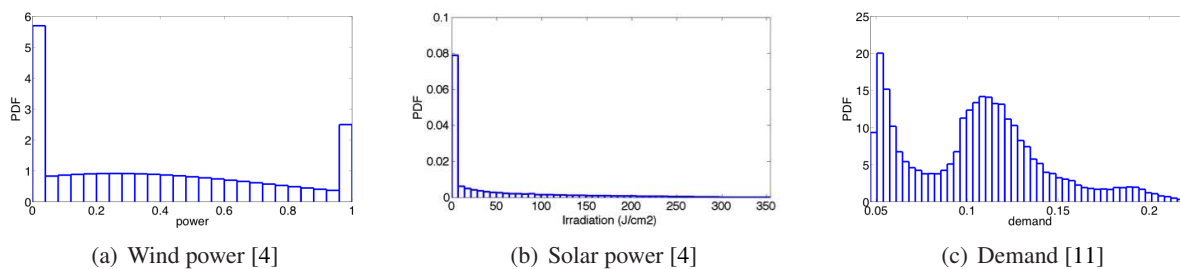


Figure 4: Input probability densities to the IEEE 300 bus test system.

sparse grids show not yet a major computational advantage in this three-dimensional example, although they give more flexibility in choosing the number of points. The input uncertainties cause significant uncertainty in the branch current with substantial tail probabilities.

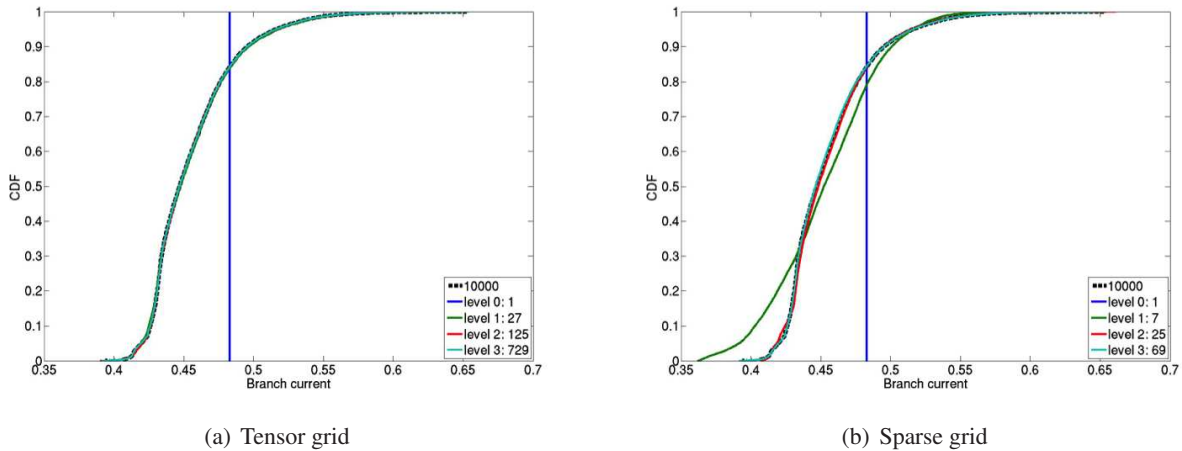


Figure 5: Cumulative probability distribution function of the current in branch number 1.

4.0 NUCLEAR REACTOR SAFETY FLOW

Nuclear Reactor Safety (NRS) analysis requires high-fidelity Computational Fluid Dynamics (CFD) simulations. Systematic Verification & Validation (V&V) of the CFD simulations is increasingly demanded by the safety regulators. Concerning the validation of the applied CFD methods, Uncertainty Quantification (UQ) is essential for the quantitative comparison of the numerical results with the measurement uncertainties. The main topics for the application of UQ to CFD in NRS include the characterization of uncertainty sources in an uncertainty term breakdown and the employed UQ methods. An example is the application of UQ to the validation of Unsteady Reynolds-Averaged Navier-Stokes (URANS) computations for inherent Boron Dilution Transients (BDT) [5]. There are different sources of uncertainty that result in different realizations for repeated numerical simulations with small disturbances in BDT. These are the numerical uncertainty in the selection of the spatial grid size, parametric uncertainty in the geometrical corner sharpness, fluid densities, and mass flow rates, as well as model uncertainties in the turbulence model.

The ASME V&V 20-2009 framework [8] is a standard for model validation. Validation is based on the comparison of experimental validation data D with simulation results S , see Figure 6. Its objective is to isolate and estimate the model uncertainty by quantifying all other uncertainties.

These uncertainties include the experimental uncertainty δ_D reported by experimentalists. The ROCOM BDT experiment the uncertainties originate from the wire mesh sensors and the statistical noise of the limited number of only 10 realizations of the experiment. Numerical uncertainties δ_{num} can be quantified using numerical error estimation techniques. In the ROCOM simulations three hexahedral meshes are used with $1.5 \cdot 10^6$, $6 \cdot 10^6$, and $24 \cdot 10^6$ cells to estimate the numerical error.

The parametric input uncertainties δ_{input} in the fluid densities and the mass flow rates are propagated using a Stochastic Collocation approach to limit the analysis to a realistic number of 20 samples in the framework from [14]. The nested parametric uncertainty propagation and numerical error estimation in that approach are decoupled here to reduce the computational costs. The numerical error estimation is performed at the mean input parameter values and the uncertainty propagation is performed on the medium spatial mesh, which has been found to be sufficient. Combining the experimental and numerical results with the experimental uncertainty, numerical error, and parametric uncertainty will lead to an estimate of the model uncertainty, with which the model can be validated.

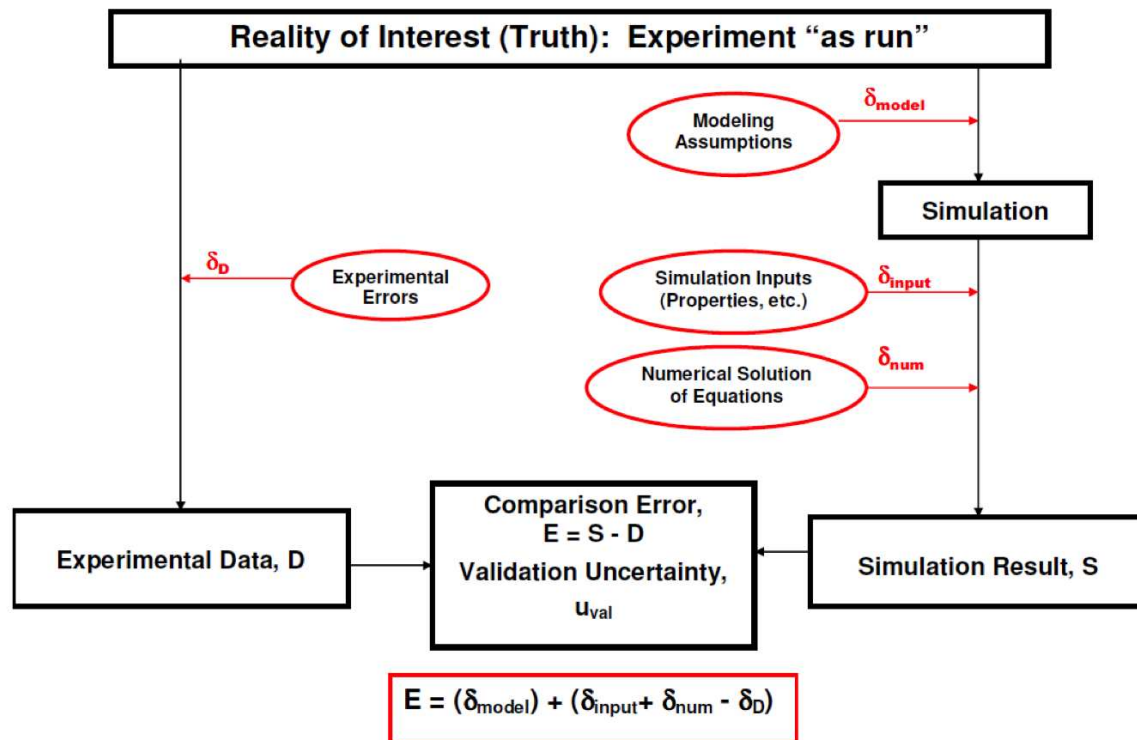


Figure 6: ASME V&V 20-2009 diagram for model validation [8].

5.0 WIND ENGINEERING

Uncertainty plays a significant role in the Benchmark on the Aerodynamics of a Rectangular Cylinder (BARC) with a chord-to-depth ratio of 5, see Figure 7. Despite the relatively straightforward geometry, the BARC case contains most difficulties also found in realistic bluff body flows of interest in wind engineering. The flow around the stationary elongated cylinder is turbulent with unsteady separation and reattachment at the considered high Reynolds number of 40,000. The objective of the BARC benchmark is to collect different data sets for assessing the reliability and the dispersion of computational and experimental studies [1]. The comparison of these results revealed that both the numerical simulations as well as the wind tunnel tests are impacted by various sources of uncertainty. In particular, besides modeling uncertainties and numerical errors, in numerical simulations it is difficult to exactly reproduce the experimental conditions due to uncertainties in the set up parameters, which sometimes cannot be exactly controlled or characterized.

In this study, a computational sensitivity analysis and uncertainty quantification (UQ) study to the parametric uncertainties is carried out using probabilistic methods. The following uncertain set-up parameters are investigated in the subsequent uniform ranges: the angle of incidence α ($0^\circ - 1^\circ$), the longitudinal turbulence intensity I_x ($0 - 0.05$), and the turbulence length scale L ($1D - 5D$), with cylinder thickness D . All these parameters have significant effects on the flow features and on the aerodynamic loads and they are often not characterized or difficult to be exactly controlled in experiments. Sensitivity analysis to small variations of the angle of incidence is also done, because it is interesting to highlight to which extent this affects the symmetry

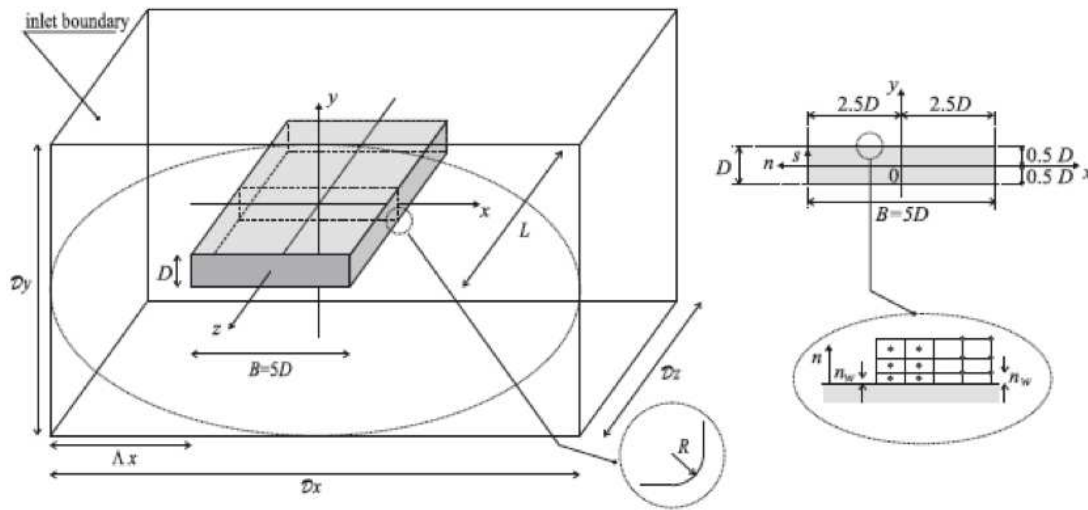


Figure 7: BARC model and domain geometry for the computational study [1].

of the flow.

The computations are performed using 2D URANS simulations in order to make the computational effort feasible. The SST $k - \omega$ URANS model is used that has proven to give good results for the BARC case [1]. The numerical error is estimated by comparing the results from computations on different mesh sizes. This step employs the experience and the spatial meshes from earlier studies [2, 3]. Among the output quantities of interest are the bulk parameters: time-average and Root Mean Square (RMS) of the vertical c_y and horizontal c_x force coefficients, and the nondimensionalized frequency in terms of the Strouhal number St . In addition, the statistics of the time-averaged pressure coefficient distribution in terms of the mean and standard deviation.

The Stochastic Collocation (SC) method [15] is employed to perform the probabilistic uncertainty propagation of the three set-up parameters. This results in 25 URANS simulations based on the sparse grid extension of the level-2 Clenshaw-Curtis quadrature points. The UQ propagation error is estimated by comparing the results with those on the nested lower levels. The result is a probabilistic comparison of the impact of the considered errors and uncertainties as well as quantitative recommendations for future research directions within the BARC benchmark.

The convergence of the uncertainty standard deviation of the bulk parameters is given in Table 2 for the fine mesh as function of the sparse grid level and the number of Computational Fluid Dynamics (CFD) simulations. The considered parameters have the largest impact on $mean(c_y)$ and $RMS(c_y)$. This is mainly caused by the uncertainty in the angle of attack α . These sensitivities are in agreement with previous BARC findings which indicate that this is the most dispersed parameters.

Table 2: Uncertainty standard deviation of the bulk parameters on the fine mesh.

level	points	mean(c_y)	mean(c_x)	RMS(c_y)	RMS(c_x)	St
0	1	0	0	0	0	0
1	7	0.24000	0.00349	0.02775	0.01216	0
2	25	0.23653	0.00282	0.02460	0.00869	0

The surface pressure coefficient along the cylinder surface coordinate s is given in Figure 8 averaged over the upper and the lower side. In Figure 8 the level is fixed at 2 and the coarse and fine mesh results are compared. The figures show the mean \pm the standard deviation. The considered parameters have the largest impact on $\text{RMS}(C_p)$. This agrees with the known BARC findings identifying this as the most uncertain output. The effect of grid refinement is in this case more important than that of the considered parameters in Figure 8. This is caused by the coarseness of the first grid. The results do not change when lowering the UQ level, which shows a very good convergence of the UQ procedure.

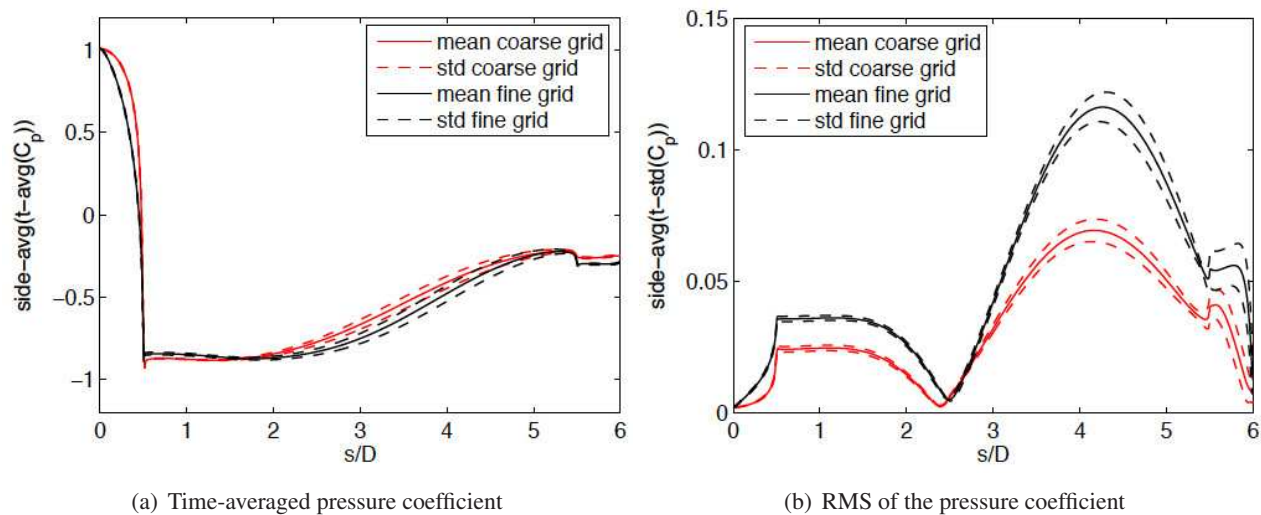


Figure 8: Side-averaged surface pressure quantities on the cylinder, level 2.

6.0 CONCLUSIONS

Non-intrusive UQ in mainly energy applications has been considered. The applications included wind turbine flow [6, 7], stochastic power flow, nuclear safety flow [5], and a wind engineering benchmark [1]. In the wind turbine case, uncertainty in the wind conditions, the surface roughness, and geometrical manufacturing uncertainties was taken into account. Wind uncertainty reduced the power output by half compared to the deterministic performance. The design optimization of the wind turbine under the uncertainty resulted in a robust peak probability at the peak performance in the range of its probability distribution. This uncertainty originating from wind power and solar power generation flows into the electrical power grid in combination with the uncertain demand. This forms a new challenge for grid operators in addition to the typically distributed generation of renewables. Propagation of these uncertainties through the stochastic power flow equations shows that the significant tail probabilities can be accurately approximated using a level-1 tensor grid or a level-2 sparse grid with 27 and 25 samples, respectively, compared to a 10,000-sample Monte Carlo simulation.

In Nuclear Reactor Safety (NRS) flow simulations, it is instrumental to quantify the model uncertainty in a validation process. The ASME V&V 20-2009 standard allows to estimate model uncertainty by comparing the experimental and numerical results with the estimates of experimental uncertainty, numerical error, and input parameter uncertainty. For the ROCOM Boron Dilution Transient (BDT) experiment, the experimental uncertainty is caused by the wire mesh sensors and the limited number of 10 realizations. The numerical error is estimated using three different mesh sizes and the parametric uncertainty is propagated with a Stochastic

Collocation approach. Parametric uncertainty and numerical error estimation are decoupled to make the study feasible.

The wind engineering example around the rectangular 5:1 BARC cylinder considered uncertainty in the angle of incidence, the longitudinal turbulence intensity, and the turbulence length scale. The results agreed with the known BARC findings identifying the mean and RMS of the vertical force coefficient, and the RMS of the surface pressure as the most sensitive outputs. The numerical error had the largest impact because of the coarseness of the smallest grid. The UQ results showed already very good convergence for low approximation sparse grid levels.

ACKNOWLEDGMENTS

I would like to sincerely thank the following collaborators. Giovanni Petrone, Carlo de Nicola, Dominique Quagliarella, John Axerio-Cilies, and Gianluca Iaccarino for the collaboration on the wind turbine flow section. Richard de Groot, Michel Verburg, and Gabriël Bloemhof for the collaboration on the stochastic power flow section. Ed Komen and Santhosh Jayaraju for the collaboration on the nuclear safety flow section. Pejman Shoeibi Omrani, Alessandro Mariotti, Maria Vittoria Salvetti, Luca Bruno, and Nicolas Coste for the collaboration on the wind engineering section.

REFERENCES

- [1] L. Bruno, M.V. Salvetti, F. Ricciardelli, Benchmark on the aerodynamics of a rectangular 5:1 cylinder: and overview after the first four years of activity, *Journal of Wind Engineering and Industrial Aerodynamics*, Vol. 126, 2014, pp. 87–106.
- [2] L. Bruno, N. Coste, and D. Fransos, Simulated flow around a rectangular 5:1 cylinder: spanwise discretization effects and emerging flow features, *Journal of Wind Engineering and Industrial Aerodynamics*, Vol. 104-106, 2012, pp. 203–215.
- [3] L. Bruno, D. Fransos, N. Coste, and A. Bosco, 3D flow around a rectangular cylinder: a computational study, *Journal of Wind Engineering and Industrial Aerodynamics*, Vol. 98, 2010, pp. 263–276.
- [4] D. Heijboer, J. Nellestijn, *Klimaatatlas van Nederland: de normaalperiode 1971-2000*, Elmar, Delft, the Netherlands, 2002.
- [5] S.T. Jayaraju, P. Sathiah, E.M.J. Komen, E. Baglietto, Large Eddy Simulation for an inherent boron dilution transient, *Nuclear Engineering and Design*, Vol. 262, 2013, pp. 484–498.
- [6] G. Petrone, C. De Nicola, D. Quagliarella, J.A.S. Witteveen, G. Iaccarino, Wind turbine performance analysis under uncertainty, 49th AIAA Aerospace Sciences Meeting, Orlando, Florida, 2011, AIAA-2011-0544.
- [7] G. Petrone, C. de Nicola, D. Quagliarella, J.A.S. Witteveen, J. Axerio-Cilies, G. Iaccarino, Wind turbine optimization under uncertainty with high performance computing, 41st AIAA Fluid Dynamics Conference, Honolulu, Hawaii, 2011, AIAA-2011-3806.
- [8] Standard for Verification and Validation in Computational Fluid Dynamics and Heat Transfer, ASME V&V 20-2009, American Society of Mechanical Engineers (ASME), 2009.

- [9] M. Suarez-Taboada, J.A.S. Witteveen, C.W. Oosterlee, L.A. Grzelak, Impact of Heston model parameters by means of uncertainty quantification, 14th International Conference on Computational and Mathematical Methods in Science and Engineering (CMMSE), Cadiz, Spain, 2014.
- [10] University of Washington Department of Electrical Engineering, Power Systems Test Case Archive, <http://www.ee.washington.edu/research/pstca/>.
- [11] M. Verburg, The impact of large-scale penetration of PV systems on the power quality and capacity of distribution networks, M.Sc. thesis, Eindhoven University of Technology, Eindhoven, the Netherlands, 2013.
- [12] J.A.S. Witteveen, G. Iaccarino, Simplex stochastic collocation with random sampling and extrapolation for nonhypercube probability spaces, *SIAM Journal on Scientific Computing*, Vol. 34, 2012, pp. A814–A838.
- [13] J.A.S. Witteveen, G. Iaccarino, Refinement criteria for simplex stochastic collocation with local extremum diminishing robustness, *SIAM Journal on Scientific Computing*, Vol. 34, 2012, pp. A1522–A1543.
- [14] J.A.S. Witteveen, K. Duraisamy, G. Iaccarino, Uncertainty quantification and error estimation in scramjet simulation, 17th AIAA International Space Planes and Hypersonic Systems and Technologies Conference, San Francisco, California, 2011, AIAA-2011-2283.
- [15] D. Xiu, J.S. Hesthaven, High-order collocation methods for differential equations with random inputs, *SIAM Journal on Scientific Computing*, Vol. 27, 2005, pp. 1118–1139.